European Journal of Advanced Chemistry Research
Vol 5 | Issue 1 | March 2024
ISSN 2684-4478

RESEARCH ARTICLE

Synthesis and Characterisation of Ag-Co-Venlafaxine-Cyclodextrin Nanorods

Ayyadurai Mani[1], Govindaraj Venkatesh[2], Perumal Senthilraja[3], and Narayanasamy Rajendiran[1,*]

ABSTRACT

Ag and Ag/Co nanoparticles containing venlafaxine/cyclodextrin (VF/CD) inclusion complexes were synthesized and analyzed by UV-Visible, fluorescence, computational technique, DSC, FTIR, XRD, FE-SEM, and TEM. Single emission was observed in α-CD and β-CD. A blue-shifted absorption and fluorescence maximum was seen in Ag/VF/CD and Ag/Co/VF/CD nanoparticles than VF/CD inclusion complex. TEM image exposed the existence of nanorods in Ag/VF/β-CD and Ag/Co/VF/β-CD. Pure VF drug shows more antibacterial activity than Ag/VF/β-CD and Ag/Co/VF/β-CD nanomaterials. Nano particle size is also measured by X-RD and TEM.

Keywords: Cyclodextrin, Inclusion complex, Nanorod, Venlafaxine.

Submitted: August 12, 2023

Published: March 12, 2024

10.24018/ejchem.2024.5.1.147

[1] *Department of Chemistry, Annamalai University, India.*
[2] *Department of Chemistry, Muthayammal Engineering College, India.*
[3] *Department of Bioinformatics, Bharathidasan University, India.*

* ***Corresponding Author:***
e-mail: drrajendiran1967@gmail.com

1. Introduction

Recent years have seen a significant increase in interest in the fields of chemistry, life science, and clinical medicine for studies on how different medicinal compounds interact with nanomaterials. The kind and strength of these interactions have an impact on biosafety, delivery efficiency, pharmacological response, therapeutic efficacy, and medication design. Because of this, research on these interactions aids in our understanding of the structural characteristics required for the bioaffinity of medicines and nanomaterials towards pharmacological activity [1]–[4].

Due to their outstanding sensitivity, quickness, theoretical underpinnings and simplicity [4]–[9], techniques like absorption and fluorescence spectroscopy, differential scanning colorimetry, FTIR, X-RD, SEM, and TEM are effective instruments for examining the interactions between drugs and nanomaterials.

The purpose of the study is to examine how the venlafaxine drug interacts with α- and β-cyclodextrin, various solvents, computational methods, silver nano, and silver/cobalt nanomaterials were investigated using various techniques. The molecular/nano characteristics of the drug entrapped into the CD cavity can be affected by constrained space and relatively non-polar behaviour of the CD cavity [10]–[18].

2. Experiments

2.1. Synthesis of Drug: CD Inclusion Complex in Solution

Various concentrations of α-CD or β-CD solution (0.1 to 1.0 $\times$ 10^{-2} M) were taken in a 10 ml standard measuring flask. The concentration of VF stock solution is 2 $\times$ 10^{-2} M. 0.2 ml of VF stock solution was added to the flasks mentioned above. The above solution was made up to 10 ml. The final concentration of the drug is 4 $\times$ 10^{-4} M.

2.2. Synthesis of Silver and Silver/Cobalt Nanoparticles

Sol-gel process has been used to produce silver nanoparticles. 0.01 M of silver nitrate was dissolved in 200 ml of deionized water, and the solution was heated for 20 to 30 minutes at 50 °C. One to two ml of 1% trisodium citrate was added to this solution. Appearance of pale yellow colour confirmed the production of Ag nanoparticle.

In the above warmed Ag nanoparticle solution (100 ml), 0.01 M cobalt sulphate solution (50 ml) was gradually added. 100 ml of Ag nano and 150 ml of Ag/Co nano solution were frozen and dried (mini-lyophilized) at −80 °C. The powder samples of Ag and Ag/Co were collected and used for additional analysis.

2.3. Synthesis of Ag/VF/CD Inclusion Complex Nanomaterials

2×10^{-3} M of VF drug (dissolved in 20 ml ethanol) was added gradually to the CD (1×10^{-2} M in 80 ml) solution. This mixture was heated at 50 °C for two hours. Then, the silver nano (0.01 M in 50 ml) was added to the above VF/CD inclusion complex solution (50 ml) and stirred one to two hours.

Similar method was used to make nanomaterial made of Ag/Co/VF/CD. 50 ml of the Ag/Co nanoparticle solution was added to the VF/CD inclusion complex (50 ml). After that, the above two solution were frozen and dried (mini-lyophilized) at −80 °C. The powder samples of Ag/VF/CD and Ag/Co/VF/CD were collected and used for further analysis.

2.4. Antibacterial Activity

Antibacterial activity of chloroquine was assessed against bacterial pathogens by the disc diffusion method. The bacterial pathogen was inoculated in nutrient broth and cultured for 1–2 hours before an antibacterial experiment. On the Muller Hinton agar plates, every bacterial strain was dispersed separately. The disc was loaded with various quantities (25 l, 50 l, 75 l, 100 l) of chloroquine or Ag/VF/CD or Ag/Co/VF/CD and then incubated for 24 hours at 37 °C. The assay was performed three times. After the incubation time was over, the zone of inhibition was measured in milli metres.

2.5. Molecular Modeling Studies

VF, CD and its inclusion complex geometry were analysed by Spartan 08 software. Most stable complexation energy was determined theoretically after the structural assembly of two orientation inclusion complexes by PM3 method (Gaussian 09W software) in the gas phase.

3. Result and Discussion

3.1. UV-Visible and Emission Spectral Studies

Absorption and emission spectral maxima of venlafaxine (VF, Fig. 1) drug was measured in α-CD and β-CD. In aqueous CD, the VF absorption wavelength appeared at 274, 224 nm. No notable changes were noticed in VF, however, the absorbance slightly raised as the α-CD and β-CD concentration increased. The occurrence of isosbestic point and the modest fluctuation in absorbance were indicators of the construction of a 1:1 inclusion complex [10]–[18].

At 300 nm, VF exhibit single emission maxima in aqueous CD. As CD concentrations rose, the intensity of the emission increased at the same wavelength indicating that the VF molecule was trapped inside the CD cavities. VF molecule absorption and emission intensities were generally under control because the CD cavity provided non-polar atmosphere of the VF molecule. As a result, emission intensities were increased [10]–[18] due to the higher stiffness of the VF.

It is known that, the existence of an isosbestic point in the absorption spectrum verifies the creation of 1:1 inclusion complex between VF and CD. The Benesi-Hildebrand relation may be used to calculate the binding constant (K) of VF:CD. From the $1/A\text{-}A_0$ vs $1/[\alpha\text{-CD}]$ and $1/[\beta\text{-CD}]$, $1/I\text{-}I_0$ vs $1/[\alpha\text{-CD}]$ and $1/[\beta\text{-CD}]$ plot, the binding constant was estimated. The negative free energy change (ΔG) values (for α-CD: abs = −12.4, flu = −10, for β-CD: abs = −13.0, flu = −12.5) suggest the binding process was thermodynamically advantageous and spontaneous at the experimental temperature.

3.2. Effect of Solvents

To understand the inclusion process, absorption and emission spectral data of VF were examined in different polarity of the solvent. Both spectral wavelength for VF is identical in the solvents and the CD solution. In both spectra, from non-polar to polar solvent bathochromic shift observed in VF molecule. VF exhibit a single emission in all solvents. Bathochromic shift reflects increased delocalization of the $-OCH_3$ group and the aromatic ring's π-cloud [19], [20].

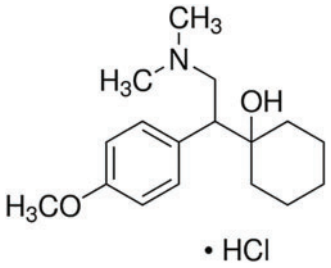

Fig. 1. Structure of venlafaxine. HCl to find the chemical structure.

3.3. Molecular Modeling

VF, α-CD, β-CD and the inclusion complexes were optimized by PM3 approach. Table I lists the HOMO and LUMO (Fig. 2), energy, enthalpy, entropy, free energy, dipole moment, zero-point vibrational energy and Mullikan charge of the free and VF:CD molecules. The above mentioned values are significantly varied in the free and VF:CD, because the CD polarity changed after VF entered into the cavity. Blue, red and green colours in HOMO-LUMO stand for nitrogen, oxygen and chlorine atoms, respectively, while green and red denote the molecules' negative and positive phases. Red colour in the molecular electrostatic potential's (MEP) figure (Fig. 2) shows that the electronegative charge of the atoms is greater than that of other atoms.

VF and CDs may create one of two distinct inclusion complexes: (i) an anisole ring may encapsulate, or (ii) a cyclohexanol ring or tertiary amine group may encapsulate in the host cavity. In VF, the horizontal bond distance is 7.02 Å and the vertical bond distance is 9.60 Å. VF vertical bond length is higher than CD cavity, hence, this drug partly encapsulated in the CD cavity. Further, partial inclusion of VF in the CD cavity was validated by the PM3 optimised structures.

3.4. Spectral Studies of the Nanoparticles

Absorption and emission spectra of the Ag and Ag/Co nanoparticles were observed in the solution phase. Transformation of colorless to yellowish solution shows the creation of Ag nano. Spherical shape was identified in Ag nano and the absorption band was noticed at 420 nm. When cobalt solution was added to Ag nano, the wavelength changed from 420, 250, 220 nm to 405, 260, 220 nm. It is generally known that the particle size, shape, and surroundings affect the plasmon resonance band's absorbance, and the quantity of nano particles does not directly correlate with the intensity of the absorption [21]. Due to surface plasmon resonance, it is known that Ag nano exhibit their highest absorption in 400–500 nm range [22].

Ag nano emission was observed at 480 nm and this wavelength moved to 470 nm when cobalt solution was added to the Ag nano. Marginal spectral signal was produced by the colloidal silver solution's distinctive colour caused by the excitation of surface plasmon vibrations during nano production [23].

Addition of VF to Ag nano, absorption wavelength red shifted from 420, 250, 220 nm to 443, 263 nm and emission moved from 480 nm to 524, 306 nm, respectively. An adding VF/CD to Ag

TABLE I: Thermodynamic Parameter Values for Venlafaxine. HCl and Its Inclusion Complexes by Semiempirical PM3 Method

Properties	VF	α-CD	β-CD	VF/α-CD	VF/β-CD
E_{HOMO} (eV)	−8.89	−10.37	−10.35	−9.23	−9.03
E_{LUMO} (eV)	0.43	1.26	1.23	0.35	2.15
$E_{HOMO} - E_{LUMO}$ (eV)	−9.32	−11.63	−11.58	−9.58	−11.18
Dipole (D)	1.20	11.34	12.29	11.44	12.76
E (kcal mol^{-1})	−104.48	−1247.62	−1457.63	−1366.29	1577.16
ΔE (kcal mol^{-1})	–	–	–	−14.19	−15.05
G (kcal mol^{-1})	−276.09	−676.37	−789.52	−956.83	1214.80
ΔG (kcal mol^{-1})	–	–	–	−4.37	−149.19
H (kcal mol^{-1})	−221.93	−570.84	−667.55	818.11	1024.80
ΔH (kcal mol^{-1})	–	–	–	−25.34	−135.14
S (kcal/mol-Kelvin)	0.181	0.353	0.409	0.565	0.493
ΔS (kcal/mol-Kelvin)	–	–	–	−0.031	−0.097
ZPE	261.23	635.09	740.56	899.83	1156.28

Note: eV-electron volt; kcal/mol-kilocalorie per mole; Kelvin-temperature in Kelvin; ZPE = Zero-point vibration energy; ΔE-difference in energy, ΔH-difference in enthalpy, ΔS-difference in entropy.

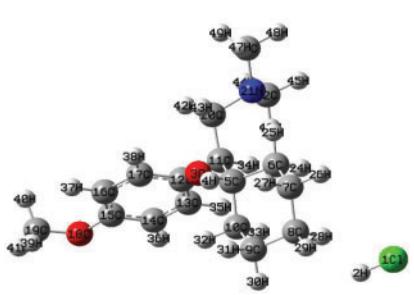

(a) Optimized structure

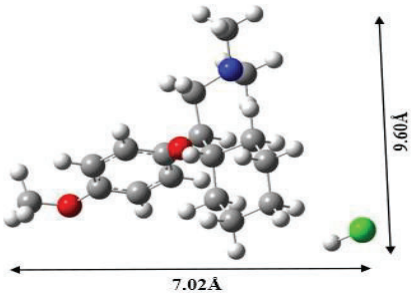

(b) Horizontal and vertical distance

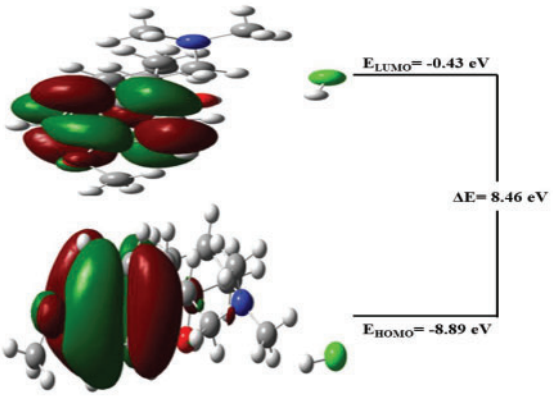

(c) HOMO, LUMO

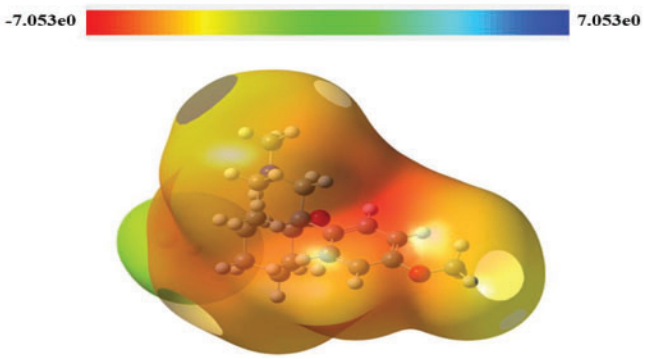

(d) MEP

Fig. 2. PM3 optimized structures of (a, b) venlafaxine. HCl (c) HOMO, LUMO and (d) MEP of VF to find the overlapping and interactions of the atoms. In HOMO-LUMO- dark green and dark red colours indicate negative and positive phase, blue-nitrogen, pale green-chlorine, pale red-oxygen, black-carbon, white-hydrogen atom.

nano, the absorption and emission maxima blue shifted to 402, 276, and 303 nm, respectively. The hypsochromic shift is seen in both spectra because the Ag nano interact with VF/CD molecules.

Upon addition of VF to Ag/Co nano, the absorption moved to 454 and 273 nm and emission maxima blue shifted to 472, 359, and 323 nm, respectively. When VF:β-CD added to Ag/Co nano, the absorption blue shifted from 405, 260, 220 nm to 367, 272 nm and emission shifted from 470 nm to 305 nm. This suggests that the Ag/Co nano encapsulated in the CD cavity. Generally, if the guest encapsulated in the CD cavity tends to rise or decrease the intensity of the inclusion complex. Their interaction is supported by spectral fluctuations.

3.5. FE-SEM and EDAX Images

Ag nano, Ag/Co nano, VF, Ag/VF/β-CD and Ag/Co/VF/β-CD were examined by FE-SEM and EDAX (Fig. 3). The photos demonstrate the morphologies of all the above nanomaterials clearly: Ag has an oyster shape, Ag/Co has a marble rack or cloud shape, Ag/VF drug has a crystal shape, Ag/VF/CD inclusion complex has a microrod shape and Ag/Co/VF/CD also has a microrod shape.

In accordance with FE-SEM-EDAX data: (a) Ag nano contains 58.31% silver nano and 41.69% oxygen; (b) Ag/Co nano contains 44.08% silver, 38.47% cobalt and 17.45% oxygen; (c) VF contains

71.47% carbon, 17.16% oxygen, 5.93% nitrogen, and 5.43% chlorine; (d) The composition of Ag/VF/β-CD is 36.15% silver, 30.67% carbon, 10.27% nitrogen, 20.61% oxygen and 2.30% chlorine; and (e) The composition of Ag/Co/VF/β-CD is 26.13% silver, 25.12% cobalt, 25.57% carbon, 10.27% nitrogen, 10.61% oxygen and 2.30% chlorine. FE-SEM pictures of Ag, Ag/Co nano, and VF are different from Ag/VF/β-CD and Ag/Co/VF/β-CD. The alteration of the morphology is evidence that new nano has formed.

3.6. TEM and EDX Images

TEM images of Ag/VF/β-CD and Ag/Co/VF/β-CD are displayed in Fig. 4. TEM pictures reveal that nanorod like microstructures found in Ag/VF/β-CD and Ag/Co/VF/β-CD. Uniformly spherical particles were seen in Ag and the size between 12 and 14 nm and Ag/Co nano size between 15 and 17 nm. However, Ag/VF/β-CD and Ag/Co/VF/β-CD nanorod sizes were displayed between 100 and 200 nm.

The formation of nanoparticles is supported by the following TEM-EDX data: (a) 38.17% silver, 28.65% carbon, 11.25% nitrogen, 19.31% oxygen and 2.28% chlorine were present in Ag/VF/β-CD; (b) 27.15% silver, 24.10% cobalt, 26.55% carbon, 9.25% nitrogen, 10.56% oxygen and 2.25% chlorine present in Ag/Co/VF/β-CD. The presence of Ag and Ag/Co along with VF/β-CD is confirmed by TEM-EDX. Further, the particles size is also measured by TEM: Ag/VF/β-CD nano size is 22.41 nm and Ag/Co/VF/β-CD nano size is 15.33 nm.

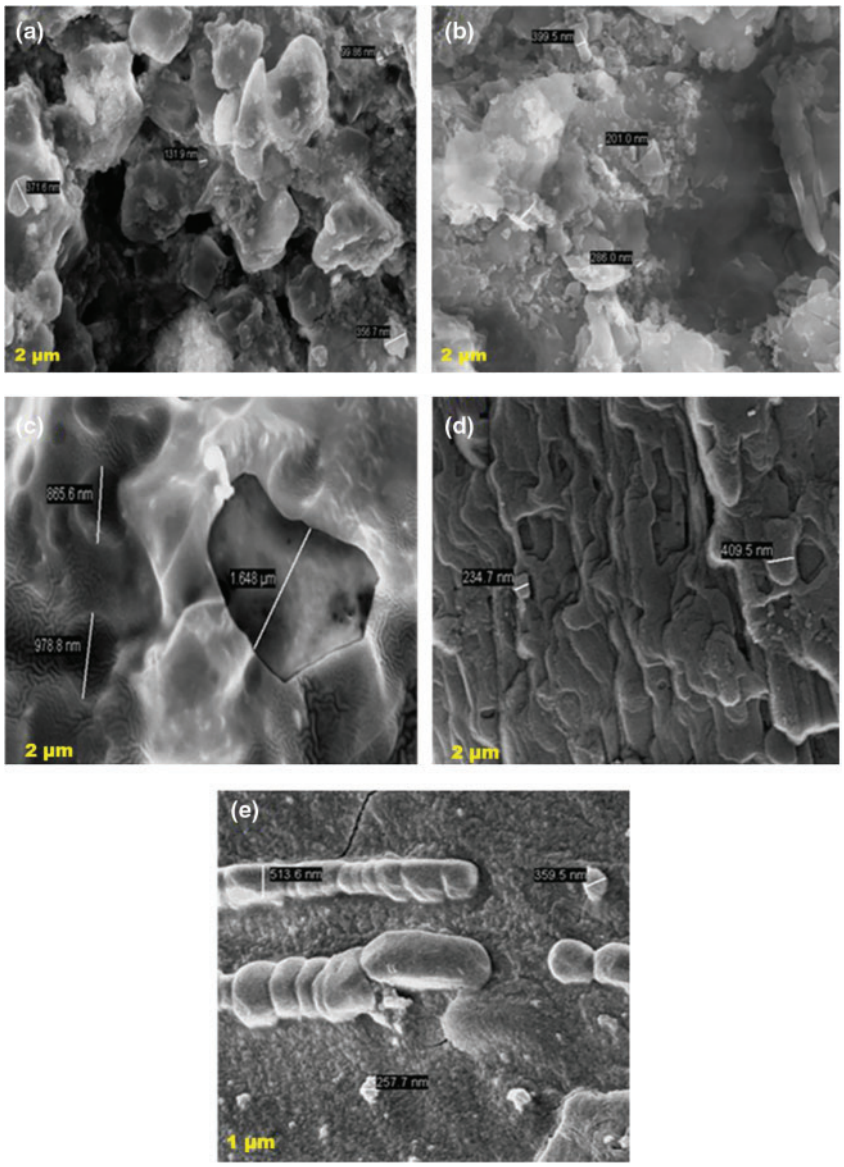

Fig. 3. FE-SEM images for (a) Ag nano, (b) Ag/Co, (c) venlafaxine. HCl, (d) Ag/VF/β-CD, (e) Ag/Co/VF/β-CD to find the morphology of the nanomaterials.

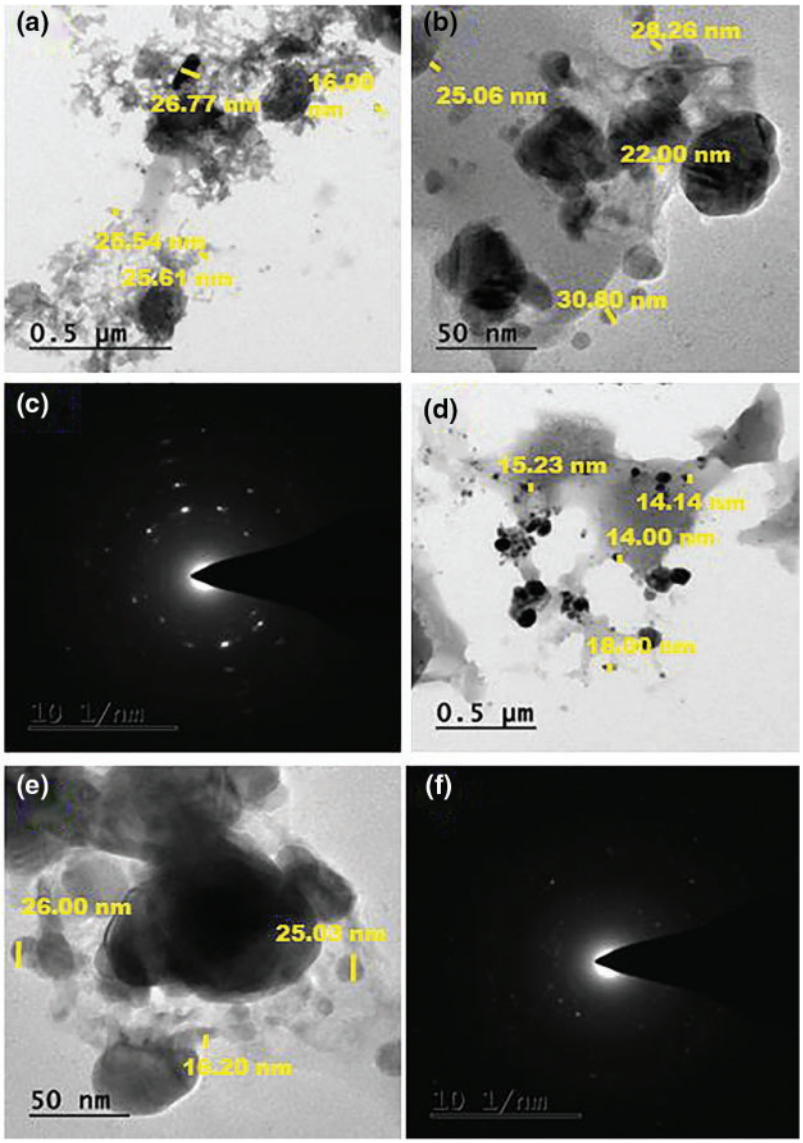

Fig. 4. TEM images for (a-c) Ag/VF/β-CD, (d-f) Ag/Co/VF/β-CD to find the nano structure of the nanomaterials.

3.7. Infrared Spectral Studies

FTIR spectra of Ag, Ag/Co nano, VF, Ag/VF/β-CD and Ag/Co/VF/β-CD are also studied. The IR frequencies observed at 3289 cm^{-1}, 2355 cm^{-1}, 1633 cm^{-1}, and 699 cm^{-1} in Ag nano, and 3242 cm^{-1}, 2435 cm^{-1}, 1641 cm^{-1}, and 675 cm^{-1} were present in Ag/Co nano. In Ag/VF/β-CD and Ag/Co/VF/β-CD, the aforementioned frequencies saw a considerable modification. In silver nano, 2355 cm^{-1} frequency represents the presence of a -C = N- bond, and 1663 cm^{-1} designates the presence of a -C-O- bond.

In VF, stretching frequency of the OH group in cyclohexanol at 3317 cm^{-1} was moved to 3265 and 3350 cm^{-1} in Ag/VF/β-CD and Ag/Co/VF/β-CD nano, respectively. The -OCH_3/-NCH_3 frequency of the VF looks at 2343 cm^{-1} and was shifted to 2350 and 3350 cm^{-1}, respectively in Ag/VF/β-CD and Ag/Co/VF/β-CD nanomaterials. The aromatic ring and C=C stretching frequency of the VF seems at 1610 cm^{-1} was moved to 1644 cm^{-1} and 1648 cm^{-1} in Ag/VF/β-CD and Ag/Co/VF/β-CD nano, respectively. The aromatic C-C stretching frequency of the VF looks at 1365 cm^{-1} and was shifted to 1351 cm^{-1} and 1380 cm^{-1} in Ag/VF/β-CD and Ag/Co/VF/β-CD nano, respectively. In VF, the C-O-C stretching frequency appears at 1232 cm^{-1} and as moved to 1156 and 1178 cm^{-1}, respectively in Ag/VF/β-CD and Ag/Co/VF/β-CD. The tertiary nitrogen frequency of the VF appearing at 495 cm^{-1} was shifted to 442 cm^{-1} and 445 cm^{-1} in Ag/VF/β-CD and Ag/Co/VF/β-CD, respectively. Compared to VF, Ag/VF/β-CD and Ag/Co/VF/β-CD nanomaterials showed marked changes in the IR frequencies suggesting that the VF/β-CD interact with the Ag, and Ag/Co nanomaterials.

3.8. DSC Thermograms

Thermal curve of pure VF, Ag, Ag/Co nano, Ag/VF/β-CD, and Ag/Co/VF/β-CD were measured in DSC. Three exothermic peaks were seen in the thermal curve of Ag nano at 198.8 °C, 250.2 °C, and 341.1 °C. In Ag/Co nano, three exothermic peaks appear at 180.4 °C, 205.3 °C, and 290.3 °C whereas VF drug exhibits two endothermic peaks at 218.2 °C and 277.5 °C.

Two endothermic peaks appear in Ag/VF/β-CD nano at 121.7 °C and 166.6 °C and one exothermic peak at 318.4 °C. In Ag/Co/VF/β-CD nano, two endothermic peaks can be seen at 126.3 °C and 171.2 °C, while one exothermic peak at 318.6 °C. The endothermic peaks in the inclusion of complex nanomaterials are caused by the loss of water from the CDs. In contrast to pure VF, Ag and Ag/Co, different peak arises in the Ag/VF/β-CD and Ag/Co/VF/β-CD nanomaterials.

3.9. Powder X-Ray Diffractograms

XRD approach provided additional confirmation of the creation of nanomaterials. With the use of the JCPDS data, the mineral name (3C) and the development of face-centered cubic (FCC) structure have been confirmed. JCPDS card number 87-0717 was used to index of the diffraction peaks with its standard Ag nano face-centered cube peaks. The values of the hkl plane are found at 111, 200, 220, and 311, respectively.

Four distinct powder peaks for Ag nano emerge at $2\theta° = 38.11°$, 44.30°, 64.45° and 77.40°. Six peaks are shown in Ag/Co nano at $2\theta° = 11.34°$, 18.15°, 22.90°, 31.85°, 36.05°, and 64.75°.

In Ag/VF/β-CD nano, there are fifteen peaks that can be seen on $2\theta° = 8.73°$, 10.89°, 16.59°, 17.38°, 22.75°, 25.64°, 26.24°, 30.76°, 33.13°, 35.49°, 37.85°, 40.81°, 43.35°, 64.22°, and 77.20°. There are fourteen peaks noted in Ag/Co/VF/β-CD nano on $2\theta° = 10.33°$, 12.10°, 15.05°, 18.98°, 20.37°, 22.34°, 26.66°, 31.78°, 34.32°, 37.88°, 43.77°, 45.91°, 64.02° and 77.07°.

Nano particles size is also measured in X-RD by Sheerer method: Ag nano–16.14 nm, Ag/Co–16.56 nm, Ag/VF/β-CD nano–17.70 nm, and Ag/Co/VF/β-CD nano–14.46 nm. Compared to isolated VF, XRD patterns of Ag/VF/β-CD and Ag/Co/VF/β-CD nano showed a clear diffraction pattern supporting that new nanomaterials were formed. Further, a number of prominent peaks appeared in the 10 to 80 degree range conforming to the formation of Ag/VF/β-CD and Ag/Co/VF/β-CD nanomaterials.

3.10. Antibacterial Results

Antibacterial activity of six bacterial organism was examined in VF, Ag/VF/β-CD, Ag/Co/VF/β-CD, and drug samples. Except *Staphylococcus aureus*, isolated VF drug is active in the remaining five pathogens, however, Ag/VF/β-CD is active only one pathogen, and Ag/Co/VF/β-CD is active in two pathogens.

Antibacterial activity of isolated VF against the six pathogens are given: *Escherchia coli* ~22 mm; *Leucobacteralbus* ~23 mm; *Bacilus pumilis* ~ 15 mm; *Bacilus* subtilis ~10 mm; *salmonella typhi* ~8 mm and VF is inactive in *Staphylococcus aureus* (zero mm).

Ag/VF/β-CD is active only in *salmonella typhi (*8 mm) and Ag/Co/VF/β-CD is active *Bacilus* subtilis (10 mm) and *salmonella typhi* (8 mm). Antibacterial activity results revealed that the isolated VF drug is shows more antibacterial activity than Ag/VF/β-CD and Ag/Co/VF/β-CD.

4. Conclusion

Different spectral, computational, and microscopy techniques were used to analyse Ag/VF/β-CD and Ag/Co/VF/β-CD nanomaterials. Ag and Ag/Co nano interactions with VF/CD inclusion complexes were validated by every experimental finding. Single emission was noticed in CD and solvents. Microscopic image showed nanorods are formed in Ag/VF/β-CD and Ag/Co/VF/β-CD. Nano size is also measured by X-RD and TEM methods. Antibacterial activity results revealed that the isolated VF drug is shows more antibacterial activity than Ag/VF/β-CD and Ag/Co/VF/β-CD.

Acknowledgment

This work was supported by the RUSA PHASE -2.0 (No. 128/A1/RUSA 2.0, Health and Environment) New Delhi, India. One of the authors, Ayyadurai Mani is thankful to the RUSA, New Delhi, India for the award of JRF fellowship.

Conflict of Interest

No potential conflict of interest was reported by the authors.

References

[1] Herve F, Urien S, Albengres E, Duche JC, Tillement J. Drug binding in plasma. A summary of recent trends in the study of drug and hormone binding. *Clin Pharmacokinet*. 1994;26:44–58. doi: 10.2165/00003088-199426010-00004.

[2] Koch-Weser J, Sellers EM. Binding of drugs to serum albumin (first of two parts). *N Engl J Med*. 1976;294:311–6. doi: 10.1056/NEJM197602052940605. PMID: 1107839.

[3] Koch-Weser J, Sellers EM. Drug therapy. Binding of drugs to serum albumin (second of two parts). *N Engl J Med*. 1976;294:526–31. doi: 10.1056/NEJM197603042941005. PMID: 765821.

[4] Ascoli GA, Domenici E, Bertucci C. Drug binding to human serum albumin: abridged review of results obtained with high-performance liquid chromatography and circular dichroism. *Chirality*. 2006;18:667–79. doi: 10.1002/chir.20301. PMID: 16823814.

[5] Oravcova J, Bobs B, Lindner W. Drug-protein binding studies new trends in analytical and experimental methodology. *J Chromatogr B*. 1996;677:1–28. doi: 10.1016/0378-4347(95)00425-4.

[6] Epps DE, Raub TJ, Caiolfa V, Chiari A, Zamai M. Determination of the affinity of drugs toward serum albumin by measurement of the quenching of the intrinsic tryptophan fluorescence of the protein. *J Pharm Pharmacol*. 1998;51:41–8. doi: 10.1211/0022357991772079.

[7] Bian Q, Liu J, Tian J, Hu Z. Binding of genistein to human serum albumin demonstrated using tryptophan fluorescence quenching. *Int J Biol Macromol*. 2004;34:275–9. doi: 10.1016/j.ijbiomac.2004.09.005.

[8] Lakowicz JR. *Principles of Fluorescence Spectroscopy*. New York: Plenum Press; 1983.

[9] Naveenraj S, Anandan S. Binding of serum albumins with bioactive substances—Nanoparticles to drugs. *J Photochem Photobiol C*. 2013;14:53–71. doi: 10.1016/j.jphotochemrev.2012.09.001.

[10] Rajendiran N, Mohandoss T, Venkatesh G. Investigation of inclusion complexes of sulfamerazine with α- and β-cyclodextrins: an experimental and theoretical study. *Spectrochim Acta A*. 2014;124:441–50. doi: 10.1016/j.saa.2014.01.057.

[11] Siva S, Venkatesh G, Sankaranarayanan RK, Antony Muthu Prabhu A, Rajendiran N. Absorption and fluorescence spectral characteristics of norepinephrine, epinephrine, isoprenaline, methyldopa, terbutaline and orciprenaline drugs. *Phys Chem Liq*. 2012;50:434–52. doi: 10.1080/00319104.2011.597029.

[12] Venkatesh G, Antony Muthu Prabhu A, Rajendiran N. Azonium-ammonium tautomerism and inclusion complexation of 1-(2,4-diamino phenylazo) naphthalene and 4-amino azobenzene. *J Fluoresc*. 2011;21:1485–97. doi: 10.1007/s10895-011-0835-1.

[13] Antony Muthu Prabhu A, Venkatesh G, Sankaranarayanan RK, Siva S, Rajendiran N. Azonium-ammonium tautomerism and inclusion complexation of 4-amino-2', 3-dimethyl azobenzene. *Indian J Chem*. 2010;49A:407–17.

[14] Rajendiran N, Balasubramanian T. Dual fluorescence of *N*-phenylanthranilic acid: effect of solvents, pH and β-CD. *Spectrochim Acta*. 2007;68A:867–76. doi: 10.1016/j.saa.2006.12.072.

[15] Sivakumar K, Stalin T, Rajendiran N. Dual fluorescence of diphenyl carbazide and benzanilide: effect of solvents and pH on electronic spectra. *Spectrochim Acta*. 2005;62A:991–9. doi: 10.1016/j.saa.2005.04.033.

[16] Stalin T, Anithadevi R, Rajendiran N. Spectral characteristics of ortho, meta and para-dihydroxybenzenes in different solvents, pH and β-CD. *Spectrochim Acta*. 2005;61A:2495–504. doi: 10.1016/j.saa.2004.08.024.

[17] Sankaranarayanan RK, Venkatesh G, Ethiraj J, Pattabiraman M, Saravanakumar K, Arivazhagan G, *et al.* Stepwise pesudopolyrotaxane nanostructure formation from supramolecular self-assembly by inclusion complexation of fast violet B with α- and β-cyclodextrins. *J Mol Struct*. 2022;1262:133080–89. doi: 10.1016/j.molstruc.2022.133080.

[18] Mani A, Ramasamy P, Antony Muthu Prabhu A, Rajendiran N. Investigation of Ag and Ag/Co bimetallic nanoparticles with naproxen cyclodextrin inclusion complex. *J Mol Struct*. 2023;1284:135301–10. doi: 10.1016/j.molstruc.2023.135301.

[19] Rajendiran N, Swaminathan M. Unusual spectral shifts of bis(4-amino phenyl) ether. *Bull Chem Soc Jpn*. 1996;69:2447–52.

[20] Rajendiran N, Swaminathan M. Spectral characteristics of 4-aminodiphenyl ether in different solvents and various pH. *J Photochem Photobiol A: Chem*. 1996;93:103–8.

[21] Slistan-Grijalv A, Herrera-Urbina R, Rivas-Silva JF, Ávalos-Borja M, Castillón Barraza FF, Posada-Amarillas A. Classical theoretical characterization of the surface plasmon absorption band for silver spherical nanoparticles suspended in water and ethylene glycol. *Low Dimens Syst Nanostruct, Physica E*. 2005;27:104–12. doi: 10.1016/j.physe.2004.10.014.

[22] Fayaz A, Mohammed M, Balaji K, Girilal M, Kalaichelvan PT, Venkatesan R. Mycobased synthesis of silver nanoparticles and their incorporation into sodium alginate films for vegetable and fruit preservation. *J Agric Food Chem*. 2009;57:6246–52. doi: 10.1021/jf900337h.

[23] Sastry M, Mayya KS, Bandyopadhyay K. pH dependent changes in the optical properties of carboxylic acid derivatized silver colloidal particles. *Colloids Surf A: Physicochem Eng Aspects*. 1997;127:221–8. doi: 10.1016/S0927-7757(97)00087-3.